Applied Mathematics and Computation 219 (2012) 3083–3090

Contents lists available at SciVerse ScienceDirect

Applied Mathematics and Computation

journal homepage: www.elsevier.com/locate/amc

An unconditionally stable numerical method for bimodal image segmentation

Yibao Li, Junseok Kim *

Department of Mathematics, Korea University, Seoul 136-713, Republic of Korea

ARTICLE INFO

Keywords:
Image segmentation
Level set model
Chan–Vese model
Lee–Seo model
Energy minimization
Unconditional stability

ABSTRACT

In this paper, we propose a new level set-based model and an unconditionally stable numerical method for bimodal image segmentation. Our model is based on the Lee–Seo active contour model. The numerical scheme is semi-implicit and solved by an analytical method. The unconditional stability of the proposed numerical method is proved analytically. We demonstrate performance of the proposed image segmentation algorithm on several synthetic and real images to confirm the efficiency and stability of the proposed method.

1. Introduction

Image segmentation is one of the fundamental tasks in computer vision and automatic image processing. Its goal is to divide the given image into different objects in each of which the intensity is homogeneous [1,2]. Up to now, various algorithms [3–19] have been proposed to solve the image segmentation problem. Among them, there are two widely used classical models based on the edges [3–9] or the regions [12–19]. In particular, the Chan–Vese model [13], which is a representative region-based image segmentation method, has been widely applied for various image processing applications. Their approach is based on the minimizing of the piecewise constant Mumford–Shah functional [18] by using the level set method [20]. The level set method is used to trace interfaces separating a domain into subdomains and effectively contours the image with the zero level set.

Lee and Seo pointed out that the energy functional of the Chan–Vese method has no minimizer [17]. Therefore it is difficult to set a termination criterion on the algorithm. To resolve the problem, Lee and Seo proposed a new mathematical model. However, they implemented their model with an explicit finite difference scheme. In practice, a stable and robust numerical algorithm is more desirable than explicit schemes. Therefore, in this paper, we propose a new level set-based model which can be solved by an accurate and unconditionally stable semi-implicit method.

This paper is organized as follows. In Section 2, a brief review of previous and our proposed models for image segmentation is given. We also describe our proposed numerical method and prove its unconditional stability. In Section 3, we present various image segmentation experiments on synthetic and real images using the proposed model and numerical method. Finally, conclusions are drawn in Section 4.

2. Description of the previous and the proposed models

In this section, we briefly review the Mumford–Shah, the Chan–Vese, and the Lee–Seo models for image segmentation. Then we propose a computationally efficient model and prove the unconditional stability of the proposed numerical scheme.

* Corresponding author.
E-mail address: cfdkim@korea.ac.kr (J. Kim).
URL: http://math.korea.ac.kr/~cfdkim/ (J. Kim).

0096-3003/$ - see front matter © 2012 Elsevier Inc. All rights reserved.
http://dx.doi.org/10.1016/j.amc.2012.09.038

2.1. Mumford–Shah model

The Mumford–Shah model is an energy-based method proposed by Mumford and Shah via an energy functional [18]. Let $\Omega \subset \mathbf{R}^2$ be the two dimensional image domain and f_0 be a given image on Ω. Then we want to find the smooth and closed finite set of segmenting curves C and f which is the piecewise smooth approximation to f_0 through the minimization of the following Mumford–Shah energy functional:

$$\mathcal{E}^{\mathrm{MS}}(f, C) = \mu|C| + \int_{\Omega} |f_0(\mathbf{x}) - f(\mathbf{x})|^2 d\mathbf{x} + \nu \int_{\Omega \setminus C} |\nabla f(\mathbf{x})|^2 d\mathbf{x}, \tag{1}$$

where $|C|$ is the length of the curve, μ and ν are positive parameters. The first term in Eq. (1) regularizes the contour by penalizing the arc length, the second is the data fitting term, and the third is the smoothing term.

Theoretical results of existence and regularity of minimizers of Eq. (1) can be found in Mumford and Shah [18]. In practice, it is not easy to minimize the Mumford–Shah energy functional because of the unknown curve C and the non-convexity of the functional, which may have multiple local minima [21].

2.2. Chan–Vese model

To overcome the difficulties in solving the Mumford–Shah functional, Chan and Vese proposed the following energy functional:

$$\mathcal{E}^{\mathrm{CV}}(c_1, c_2, C) = \mu|C| + \lambda_1 \int_{\mathrm{inside}(C)} |f_0(\mathbf{x}) - c_1|^2 d\mathbf{x} + \lambda_2 \int_{\mathrm{outside}(C)} |f_0(\mathbf{x}) - c_2|^2 d\mathbf{x}, \tag{2}$$

where λ_1 and λ_2 are positive parameters [13]. The constants c_1 and c_2 are the averages of f_0 inside and outside of C, respectively. And then Chan and Vese replaced the unknown curve C by the level-set function $\phi(\mathbf{x})$,

$$\phi(\mathbf{x}) = \begin{cases} dist(\mathbf{x}, C) & \text{if } \mathbf{x} \in \text{inside } C, \\ 0 & \text{if } \mathbf{x} \in C, \\ -dist(\mathbf{x}, C) & \text{if } \mathbf{x} \in \text{outside } C, \end{cases} \tag{3}$$

where $dist(\mathbf{x}, C)$ is the smallest Euclidean distance from $\mathbf{x}$ to the points in C. Then the energy functional $\mathcal{E}^{CV}(c_1, c_2, C)$ can be rewritten as

$$\mathcal{E}^{CV}(c_1, c_2, \phi) = \mu \int_{\Omega} \delta_\epsilon(\phi(\mathbf{x}))|\nabla\phi(\mathbf{x})| d\mathbf{x} + \lambda_1 \int_{\Omega} |f_0(\mathbf{x}) - c_1|^2 H_\epsilon(\phi(\mathbf{x})) d\mathbf{x} + \lambda_2 \int_{\Omega} |f_0(\mathbf{x}) - c_2|^2 (1 - H_\epsilon(\phi(\mathbf{x}))) d\mathbf{x}, \tag{4}$$

where H_ϵ and δ_ϵ are the regularized approximations of the Heaviside and the Dirac delta functions, respectively and are defined as

$$H_\epsilon(z) = \frac{1}{2} + \frac{1}{\pi} \arctan\left(\frac{z}{\epsilon}\right) \quad \text{and} \quad \delta_\epsilon(z) = \frac{\epsilon}{\pi(\epsilon^2 + z^2)}. \tag{5}$$

The constants c_1 and c_2 represent the mean intensity values inside and outside the contour C, respectively and are defined as:

$$c_1 = \frac{\int_\Omega f_0(\mathbf{x}) H_\epsilon(\phi(\mathbf{x})) d\mathbf{x}}{\int_\Omega H_\epsilon(\phi(\mathbf{x})) d\mathbf{x}} \quad \text{and} \quad c_2 = \frac{\int_\Omega f_0(\mathbf{x})(1 - H_\epsilon(\phi(\mathbf{x}))) d\mathbf{x}}{\int_\Omega (1 - H_\epsilon(\phi(\mathbf{x}))) d\mathbf{x}}. \tag{6}$$

By using the gradient descent method [22], the authors got the following evolution equation:

$$\frac{\partial\phi}{\partial t} = \delta_\epsilon(\phi)\left[\mu\nabla \cdot \left(\frac{\nabla\phi}{|\nabla\phi|}\right) - \lambda_1(f_0 - c_1)^2 + \lambda_2(f_0 - c_2)^2\right]. \tag{7}$$

The level set based algorithm of Chan and Vese works well in processing images with a large amount of noise and detecting objects whose boundaries can not be defined by gradient. However, due to the continual increase in the magnitude of the value of ϕ, it becomes difficult to set a termination criterion on the algorithm [17].

2.3. Lee–Seo model

To make the solution of image segmentation become a stationary global minimum, Lee and Seo [17] proposed the following energy functional with two shifted Heaviside functions:

$$\mathcal{E}^{\mathrm{LS}}(c_1, c_2, \phi) = \lambda_1 \int_{\Omega} (f_0(\mathbf{x}) - c_1)^2 \phi(\mathbf{x}) H(\alpha + \phi(\mathbf{x})) d\mathbf{x} - \lambda_2 \int_{\Omega} (f_0(\mathbf{x}) - c_2)^2 \phi(\mathbf{x}) H(\alpha - \phi(\mathbf{x})) d\mathbf{x}, \tag{8}$$

where α is an arbitrary small positive value. Here, ϕ is multiplied to prevent from computing a local minimum and $H(\pm\phi)$ is shifted by $\mp\alpha$ to confine the range of ϕ. Then, we have the following gradient descent flow equation:

$$\phi_t = -\lambda_1(f_0 - c_1)^2[H(\alpha+\phi) + \phi\delta(\alpha+\phi)] + \lambda_2(f_0 - c_2)^2[H(\alpha-\phi) - \phi\delta(\alpha-\phi)]. \tag{9}$$

Let ϕ_{ij}^n be approximations of $\phi(i,j,n\Delta t)$, where $\Delta t = T/N_t$ is the time step, T is the final time, and N_t is the total number of time steps. Lee and Seo implemented Eq. (9) with an explicit finite difference scheme.

$$\begin{aligned}\frac{\phi_{ij}^{n+1} - \phi_{ij}^n}{\Delta t} &= -\lambda_1(f_{0,ij} - c_1)^2\left[\max(\text{sign}(\alpha + \phi_{ij}^n), 0) + \phi_{ij}^n\delta_\varepsilon(\alpha + \phi_{ij}^n)\right] \\ &\quad + \lambda_2(f_{0,ij} - c_2)^2\left[\max(\text{sign}(\alpha - \phi_{ij}^n), 0) - \phi_{ij}^n\delta_\varepsilon(\alpha - \phi_{ij}^n)\right].\end{aligned}$$

Here the $\max(a,0)$ and the $\text{sign}(a)$ functions are defined as

$$\max(a,0) = \begin{cases} a & \text{if } a \geqslant 0 \\ 0 & \text{else} \end{cases} \quad \text{and} \quad \text{sign}(a) = \begin{cases} 1 & \text{if } a \geqslant 0 \\ -1 & \text{else} \end{cases}$$

Even though the Lee–Seo model works well on many bimodal segmentation problems, there are time step size restrictions on the discrete scheme since it uses the explicit Euler's scheme.

2.4. Proposed model

The Lee–Seo model has time step constraint since it uses an explicit Euler's method. To develop an implicit scheme, we replace the Heaviside function in Eq. (9) with

$$H_c(z) = \frac{1+z}{2}.$$

Fig. 1 shows Heaviside function $H_{0.05}$ and our proposed form H_c.

Then we propose the following energy functional:

$$\mathcal{E}(c_1, c_2, \phi) = \lambda_1 \int_\Omega (f_0(\mathbf{x}) - c_1)^2\phi(\mathbf{x})H_c(1 + \phi(\mathbf{x}))d\mathbf{x} - \lambda_2 \int_\Omega (f_0(\mathbf{x}) - c_2)^2\phi(\mathbf{x})H_c(1 - \phi(\mathbf{x}))d\mathbf{x}. \tag{10}$$

The constants c_1 and c_2 are defined as:

$$c_1 = \frac{\int_\Omega f_0(\mathbf{x})H_c(\phi(\mathbf{x}))d\mathbf{x}}{\int_\Omega H_c(\phi(\mathbf{x}))d\mathbf{x}} \quad \text{and} \quad c_2 = \frac{\int_\Omega f_0(\mathbf{x})(1 - H_c(\phi(\mathbf{x})))d\mathbf{x}}{\int_\Omega (1 - H_c(\phi(\mathbf{x})))d\mathbf{x}}. \tag{11}$$

If $f_0(\mathbf{x}) \approx c_1$, then the first term in Eq. (10) is close to zero. Since $(f_0(\mathbf{x}) - c_2)^2$ is non-zero, $\phi(\mathbf{x})H_c(1 - \phi(\mathbf{x})) = (2\phi(\mathbf{x}) - \phi^2(\mathbf{x}))/2$ should be large. This can be achieved if $\phi(\mathbf{x}) = 1$. Similarly, if $f_0(\mathbf{x}) \approx c_2$, then $\phi(\mathbf{x}) = -1$.

Fig. 2(a) shows the original image f_0. White and gray regions are close to 1 and 0, respectively. Fig. 2(b-e) shows mesh plot of integrand of the first and second term in Eq. (10) with different ϕ. If $\phi(\mathbf{x}) \equiv c(\text{constant})$, then $c_1 = c_2$ from Eq. (11). Thus $(f_0 - c_1)^2 = (f_0 - c_2)^2$. In this case, since $\phi \neq -1$, the integrand of first energy term is high. Similarly, the second one is also high as $\phi \neq 1$. With these together, the whole energy functional should be minimized (see the fourth column of Fig. 2(b) and (c)). Furthermore if $\phi(\mathbf{x}) = 2f_0(\mathbf{x}) - 1$, then $c_1 = 1$ and $c_0 = 0$. Obverse the integrand of first term in Eq. (10), for every $\mathbf{x} \in \text{inside}(C)$, $f_0(\mathbf{x}) = c_1$ and for every $\mathbf{x} \in \text{outside}(C)$, $\phi(\mathbf{x}) = -1$. They make the minimizer of energy achieves (see the fourth column of Fig. 2(d)). Similar results can be concluded from the second energy term. Thus the whole energy is minimized and the segmentation evolution reaches a steady state. In the same way, $\phi(\mathbf{x}) = 1 - 2f_0(\mathbf{x})$ is also a solution to minimize Eq. (10) shown in Fig. 2(e).

From this energy functional, we have the following parabolic equation:

$$\phi_t = -\lambda_1(f_0 - c_1)^2(1 + \phi) + \lambda_2(f_0 - c_2)^2(1 - \phi) = -[\lambda_1(f_0 - c_1)^2 + \lambda_2(f_0 - c_2)^2]\phi - [\lambda_1(f_0 - c_1)^2 - \lambda_2(f_0 - c_2)^2]. \tag{12}$$

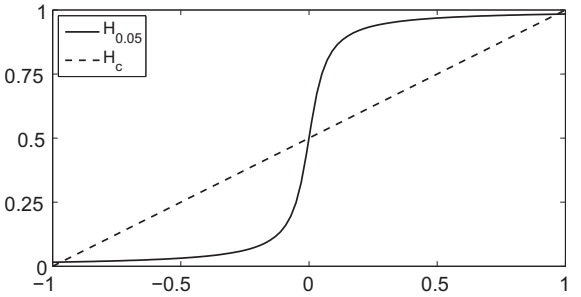

Fig. 1. Heaviside function $H_{0.05}$ and our proposed form H_c.

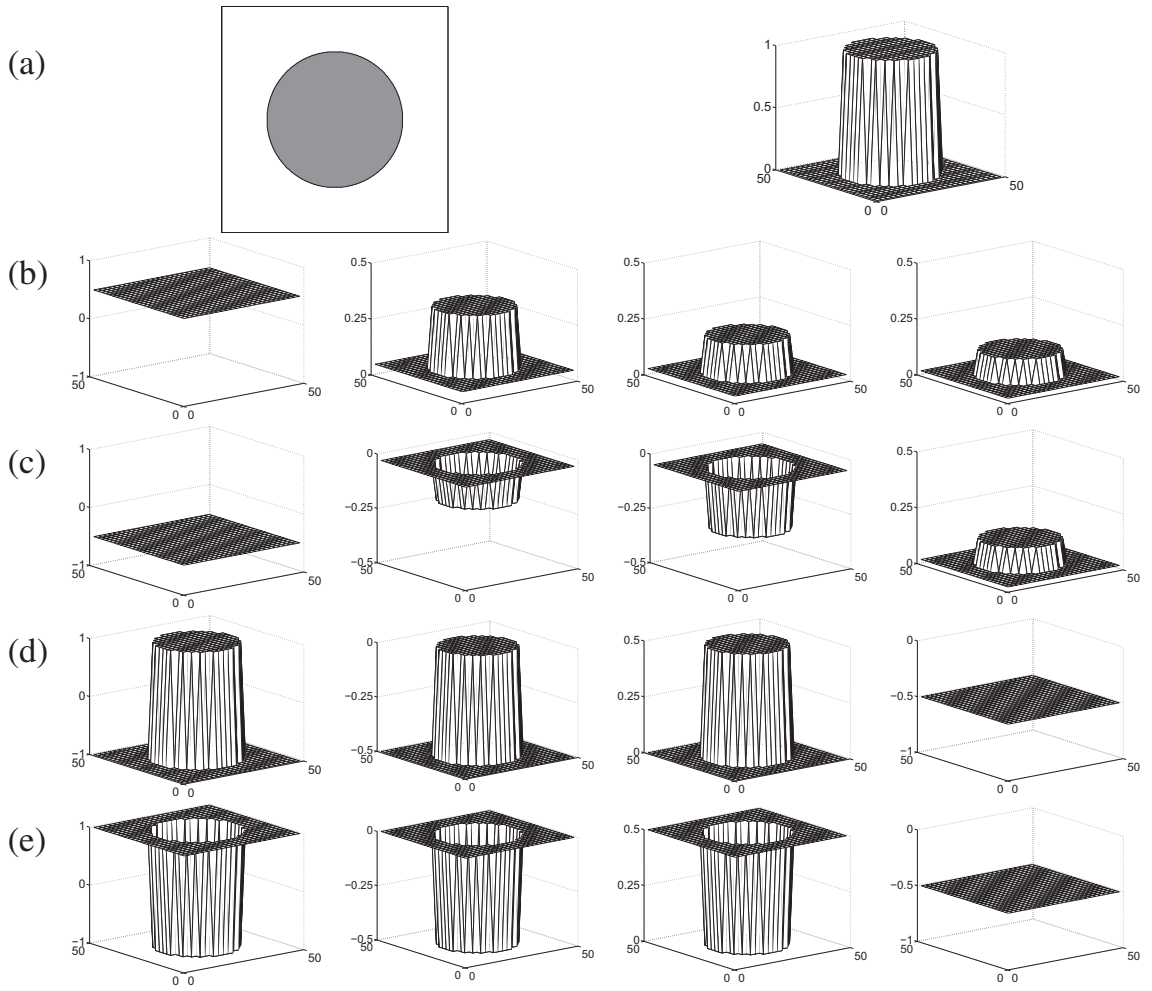

Fig. 2. (a) Original image. (b)–(e) Results with different ϕ. From left to right for columns: mesh plot of ϕ, mesh plot of the term $(f_0(\mathbf{x}) - c_1)^2\phi(\mathbf{x})H_c(1+\phi(\mathbf{x}))$, mesh plot of the term $(f_0(\mathbf{x}) - c_2)^2\phi(\mathbf{x})H_c(1-\phi(\mathbf{x}))$, and mesh plot with two terms together.

Given ϕ_{ij}^n, we want to find ϕ_{ij}^{n+1}. Let the constants c_1^n and c_2^n be defined as

$$c_1^n = \frac{\sum_i^{N_x}\sum_j^{N_y} f_{0,ij}(1+\phi_{ij}^n)}{\sum_i^{N_x}\sum_j^{N_y}(1+\phi_{ij}^n)} \quad \text{and} \quad c_2^n = \frac{\sum_i^{N_x}\sum_j^{N_y} f_{0,ij}(1-\phi_{ij}^n)}{\sum_i^{N_x}\sum_j^{N_y}(1-\phi_{ij}^n)}. \tag{13}$$

We can analytically solve Eq. (12) since it is a first-order linear differential equation. The solution at $t = (n+1)\Delta t$ is given as

$$\phi_{ij}^{n+1} = e^{-[\lambda_1(f_{0,ij}-c_1^n)^2+\lambda_2(f_{0,ij}-c_2^n)^2]\Delta t}\phi_{ij}^n + (e^{-[\lambda_1(f_{0,ij}-c_1^n)^2+\lambda_2(f_{0,ij}-c_2^n)^2]\Delta t} - 1)\frac{\lambda_1(f_{0,ij}-c_1^n)^2 - \lambda_2(f_{0,ij}-c_2^n)^2}{\lambda_1(f_{0,ij}-c_1^n)^2 + \lambda_2(f_{0,ij}-c_2^n)^2}. \tag{14}$$

When we solve time-dependent partial differential equations, stability of the numerical scheme to the equations is very important. Next, we will show our proposed numerical method is unconditionally stable. Let us assume $|\phi^n| \leqslant 1$, then from Eq. (14) we have

$$\begin{aligned} |\phi^{n+1}| &\leqslant e^{-[\lambda_1(f_0-c_1^n)^2+\lambda_2(f_0-c_2^n)^2]\Delta t}|\phi^n| + (1 - e^{-[\lambda_1(f_0-c_1^n)^2+\lambda_2(f_0-c_2^n)^2]\Delta t})\left|\frac{\lambda_1(f_0-c_1^n)^2 - \lambda_2(f_0-c_2^n)^2}{\lambda_1(f_0-c_1^n)^2 + \lambda_2(f_0-c_2^n)^2}\right| \\ &\leqslant e^{-[\lambda_1(f_0-c_1^n)^2+\lambda_2(f_0-c_2^n)^2]\Delta t}|\phi^n| + 1 - e^{-[\lambda_1(f_0-c_1^n)^2+\lambda_2(f_0-c_2^n)^2]\Delta t} \leqslant 1. \end{aligned} \tag{15}$$

Therefore the proposed scheme is unconditionally stable for any time step. Furthermore, since our model makes ϕ converges to 1 or -1, we can measure the l_2 norm error of $|\phi| - 1$ every time step, and stop the evolution when the error is smaller than a given positive value, *tol*.

3. Numerical experiments

In this section, we present numerical results using the proposed numerical algorithm on various synthetic and real images.

Let us consider a simple example which shows the basic mechanism of the proposed algorithm. $f(x,y) = 0.5 + 0.5\tanh\left(10 - 0.5\sqrt{(x-30)^2 + (y-30)^2}\right)$ is a given synthetic image and shown in the first row in Fig. 3. White and gray regions are close to 1 and 0, respectively. $\phi^0(x,y) = \tanh\left(10 - 0.5\sqrt{(x-30)^2 + (y-50)^2}\right)$ is an initial guess and is shown in the third row in Fig. 3(a). Here $\lambda_1 = \lambda_2 = 1$ and time step $\Delta t = 30$ are used. The top row shows the evolving contours overlaid on the original image. The middle and bottom rows show the right hand term of Eq. (12) and ϕ with its zero level set, respectively. Columns (a), (b), (c), and (d) are at $n = 0, 1, 2$, and 6, respectively. Observing the results in Fig. 3, the positive and negative values of the fitting term imply that ϕ moves 1 and -1, respectively. And in the steady state the segmentation curve is on the edge of the object.

In our numerical experiments, we normalize the given image f as $f_0 = \frac{f - f_{min}}{f_{max} - f_{min}}$, where f_{max} and f_{min} are the maximum and the minimum values of the given image, respectively. Hence $f_0 \in [0, 1]$. Since solutions with the proposed numerical scheme are almost insensitive to the initial configuration of ϕ, we simply initialize $\phi = 2f_0 - 1$. In this section, $tol = 0.1$ through all the numerical tests.

Fig. 4 shows that our proposed model can effectively detect different objects which were described in [17]. Here we used the parameters $\lambda_1 = \lambda_2 = 1$. Since our proposed scheme is unconditionally stable, we get the converged result after only two iterations with a relatively large time step $\Delta t = 100$. The contour plot and mesh plot of the converged result are shown in Fig. 4(b) and (c), respectively. As can be seen that the agreement between the area and image segmentation is obviously. Using the Lee–Seo model, we run the computation with the same parameters and the result is shown in Fig. 4(d). Suffering from the time restriction, the Lee–Seo model can not get the converged state with large time step.

In Fig. 5(a), we use 1 iteration to solve the image segmentation problem, which is much smaller than the method in [23], which used 835 iterations. Here, time step $\Delta t = 100$ and $\lambda_1 = \lambda_2 = 1$ are used. Fig. 5(b) shows the segmentation of watershed image. This computational experiments are set by using the same parameters as Fig. 5(a). As can be seen, image segmentations are successfully done only after 1 iterations. Next computational experiment is from [24] for contouring the image boundary of multiphase flows shown in Fig. 5(a). Using the parameters $\lambda_1 = \lambda_2 = 1$ and $\Delta t = 20$, we run the computation with only about three iterations. Since our initial condition is close to an equilibrium solution and proposed scheme is unconditionally stable, our method is very fast. Furthermore, comparing to the results shown in the top row and bottom row of Fig. 5, the agreement between the edge of objects and image segmentation also confirms the efficiency of the proposed method.

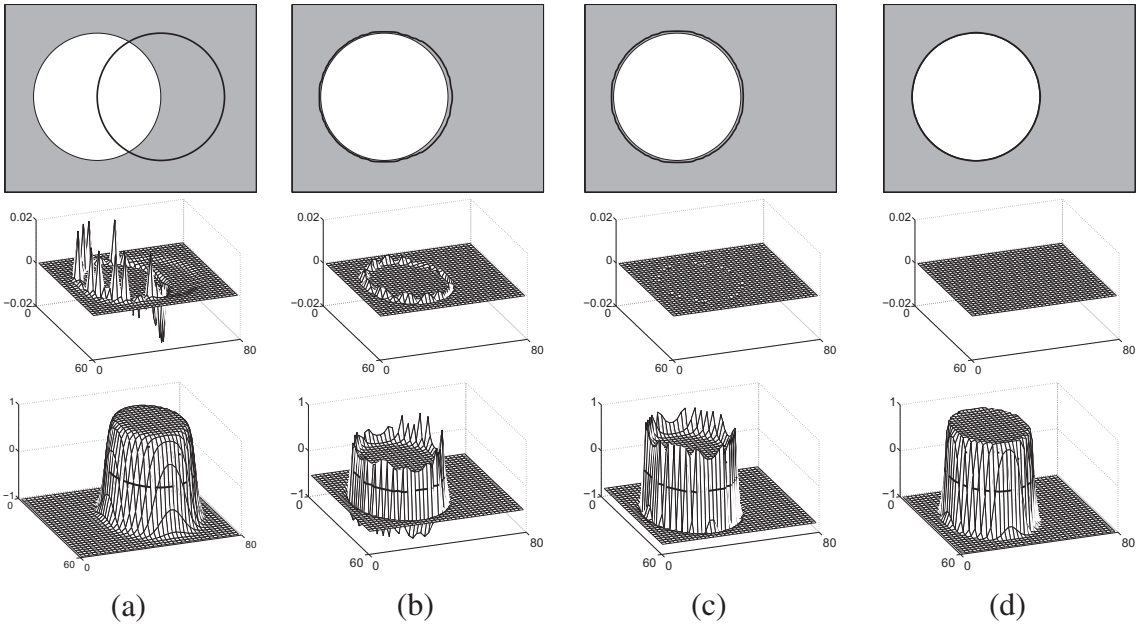

Fig. 3. Synthetic image segmentation using the proposed method. Top: the evolution of the zero level set of ϕ. Middle: the evolution of the right hand side term of Eq. (12), i.e., $\lambda[(1-\phi^{n+1})(f_0 - c_2^n)^2 - (1+\phi^{n+1})(f_0 - c_1^n)^2]$. Bottom: the evolution of ϕ and its zero level set. Columns (a), (b), (c), and (d) are at $n = 0, 1, 2$, and 6, respectively.

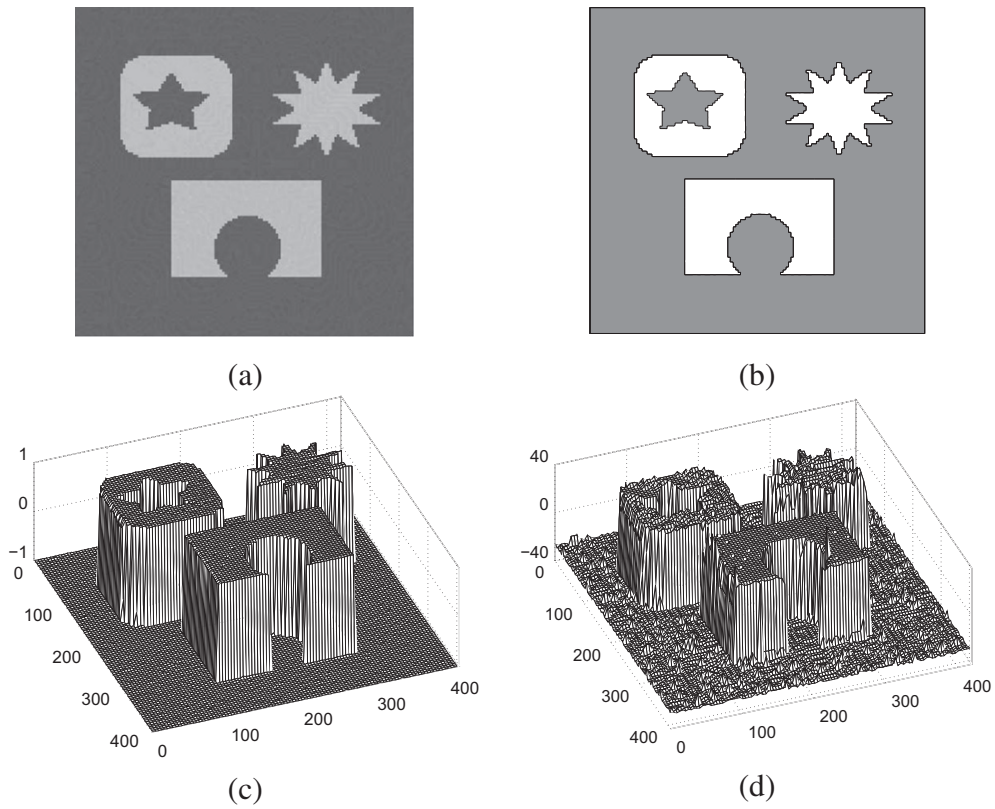

Fig. 4. Segmentation of different objects. Image size = 420 × 409. (a) Original image (b) Finial segmentation result. (c) Result using our proposed model. (d) Result using the Lee–Seo model.

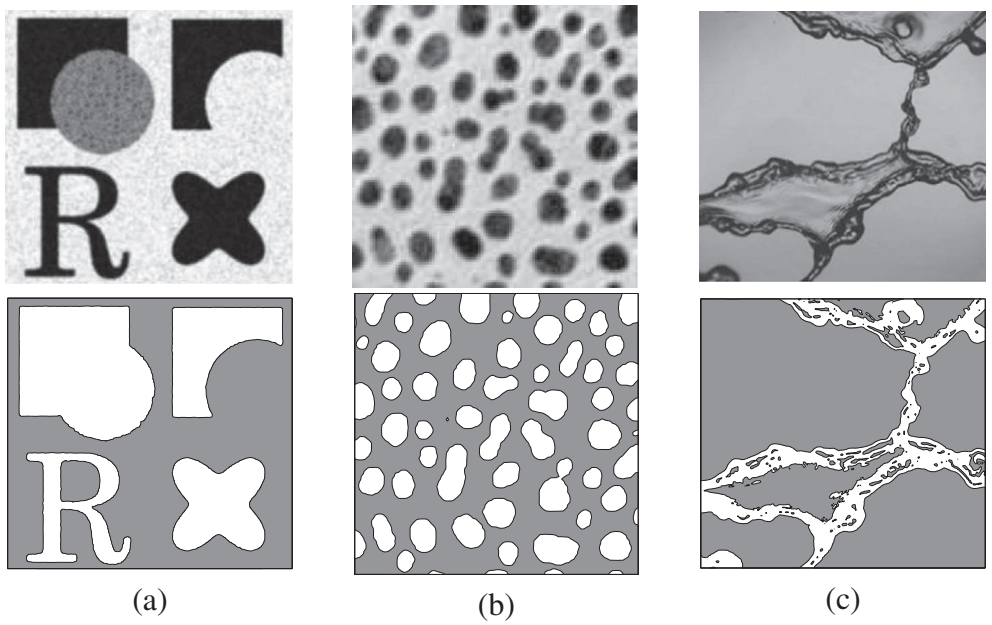

Fig. 5. Top row: original images. Bottom row: converged results. (a) Image experiment in [23]. Size = 626 × 595. (b) Watershed image. Size = 111 × 110. (c) Computational experiment in [24]. Size = 425 × 402.

As we known the gradient-based active contour model which bases on the edge-function cannot detect the smooth boundary of blurred image, however the Chan–Vese model and the Lee–Seo model can obtain a smooth one [13,17]. Here we also consider a test with our model. The initial image with image size 360×288 is presented in Fig. 6(a). To obtain a different segmentation of image, we choose different values of λ. In Fig. 6(b), we use $\lambda_1 = 0.1,\ \lambda_2 = 1$ and $\lambda_1 = 1,\ \lambda_2 = 0.1$, respectively. As can be seen, the proposed model segments the image well. Note that in both two cases, using larger time step $\Delta t = 100$, our proposed method take only two iterations, which is much smaller than the Lee–Seo method, which used 24 iterations with smaller time step $\Delta t = 0.5$ for time step restriction.

Fig. 7 shows the performance results of the proposed method on medical images. The segmentation result for a real blood vessel (left anterior descending) image is presented in Fig. 7(a). Here $\Delta t = 10,\ \lambda_1 = 1$ and $\lambda_2 = 0.5$ are used. It took three iterations. Fig. 7(b) shows the segmentation of cell image. $\Delta t = 100$ and $\lambda_1 = \lambda_2 = 1$ are used and it took two iterations. In Fig. 7(c), the segmentation of brain MR image is shown. $\lambda_1 = 1$ and $\lambda_2 = 0.5$ are used and it took two iteration with the time step $\Delta t = 15$.

Next, time step, total iterations, and CPU time in second for Fig. 7 are compared with the Lee–Seo model in Table 1. Tests were performed on a 3 GHz Intel Pentium with 3 GB of RAM loaded with MATLAB 2009[25]. As can be observed from Table 1, our proposed method yields faster results than the Lee–Seo approach. Since our method is unconditional stable, we can solve the image segmentation problem with large time step. Thus our method is robust and efficient.

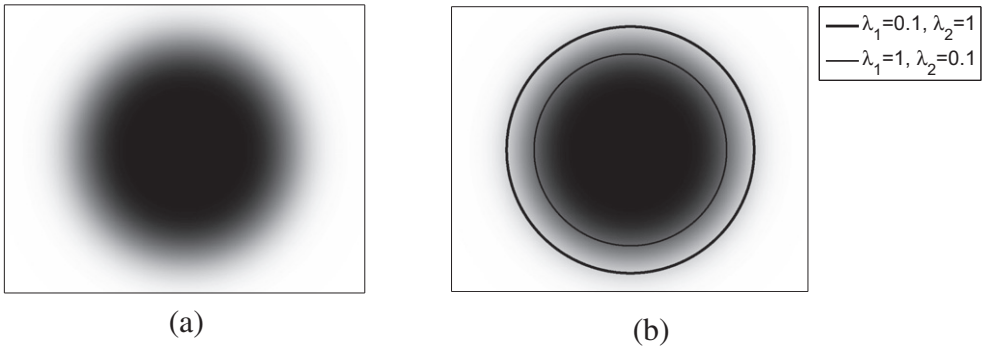

Fig. 6. Results of our method for blurred image. Size $= 360 \times 288$. (a) Original images. (b) Final segmentation results with different λ values.

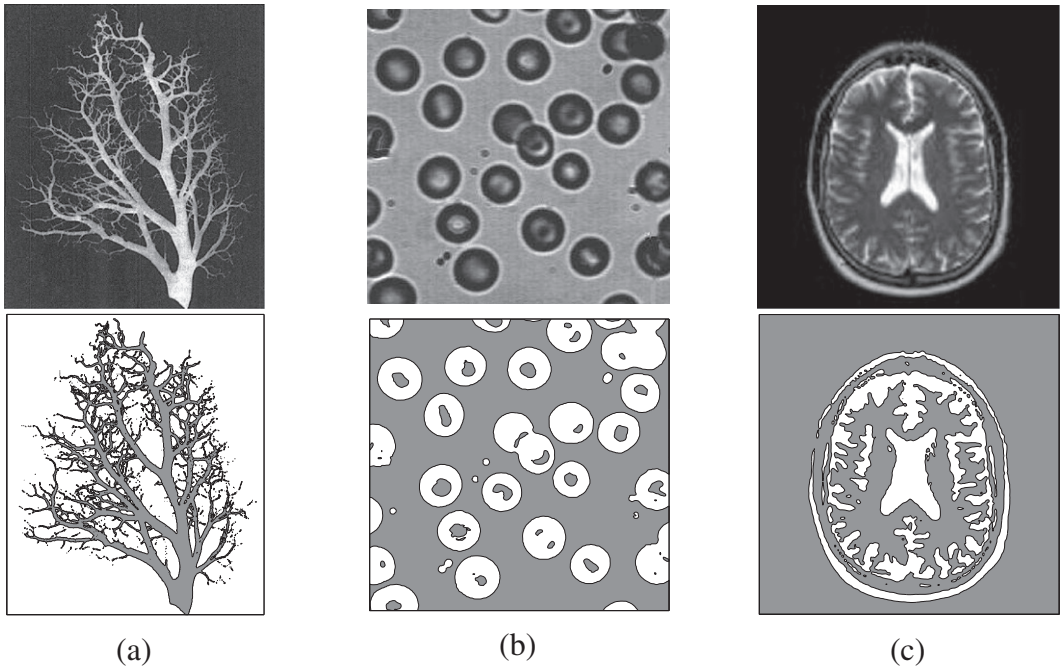

Fig. 7. Medical image segmentations. Top row: original images. Bottom row: converged results. (a) Blood vessels image with size $= 600 \times 514$. (b) Cell image with size $= 272 \times 262$. (c) Brain MR image with size $= 350 \times 350$.

Table 1
Time step, iterations, and CPU time (second) for our proposed method and the Lee–Seo model in segmenting images in Fig. 7.

	Fig. 7(a)			Fig. 7(b)			Fig. 7(c)		
	Δt	Iteration	Time	Δt	Iteration	Time	Δt	Iteration	Time
Our method	10	3	0.203	100	2	0.031	15	2	0.047
Lee–Seo	0.5	30	2.094	0.5	51	1.078	0.5	68	2.328

4. Conclusion

In this paper, we proposed a new level set-based model and an unconditionally stable numerical method for bimodal image segmentation. Our model is based on the Lee–Seo active contour model. The numerical scheme is semi-implicit and solved by an analytical way. An unconditional stability of the proposed numerical method was proved analytically. Since our initial condition was close to an equilibrium solution and proposed scheme was unconditionally stable, our method was very fast compared with the pervious methods [17,23]. Furthermore, observing the results, the agreement between the edge of objects and image segmentation also confirms the efficiency of the proposed method.

Acknowledgment

This research was supported by Basic Science Research Program through the National Research Foundation of Korea (NRF) funded by the Ministry of Education, Science and Technology (No. 2011-0023794).

References

[1] G.S. Linda, C.S. George, Computer Vision, Prentice-Hall, New Jersey, 2001.
[2] X.-F. Wanga, D.-S. Huanga, H. Xua, An efficient local Chan–Vese model for image segmentation, Pattern. Recogn. 43 (3) (2010) 603–618.
[3] B. Appleton, H. Talbot, Globally optimal geodesic active contours, J. Math. Imaging Vis. 23 (1) (2005) 67–86.
[4] V. Caselles, F. Catte, T. Coll, F. Dibos, A geometric model for active contours in image processing, Numer. Math. 66 (1993) 1–31.
[5] V. Caselles, R. Kimmel, G. Sapiro, Geodesic active contours, Int. J. Comout. Vis. 22 (1) (1997) 61–79.
[6] S. Kichenassamy, A. Kumar, P. Olver, A. Tannenbaum, A. Yezzi, Conformal curvature flows: from phase transitions to active vision, Arch. Ration. Mech. Anal. 134 (1996) 275–301.
[7] Z. Liu, B. Guo, New numerical algorithms for the nonlinear diffusion model of image denoising and segmentation, Appl. Math. Comput. 11 (2006) 380–389.
[8] C. Li, C. Xu, C. Gu, M.D. Fox, Level set evolution without re-initialization: a new variational formulation, in: Proc. IEEE Conf. Computer Vision and Pattern Recognition 1 (2005) 430–436.
[9] A. Yezzi, S. Kichenassamy, A. Kumar, P. Olver, A. Tannenbaum, A geometric snake model for segmentation of medical imagery, IEEE Trans. Med. Imag. 16 (2) (1997) 199–209.
[10] H. Zhao, F. Dai, J. Zhao, The application of resonance algorithm for image segmentation, Appl. Math. Comput. 194 (2007) 453–459.
[11] J.B. Mena, J.A. Malpica, Color image segmentation based on three levels of texture statistical evaluation, Appl. Math. Comput. 161 (2005) 1–17.
[12] T.F. Chan, S. Esedoglu, M. Nikolova, Algorithms for finding global minimizers of image segmentation and denoising models, SIAM J. Appl. Math. 66 (5) (2006) 1632–1648.
[13] T. Chan, L. Vese, Active contours without edges, IEEE Trans. Image Process. 10 (2) (2001) 266–277.
[14] S. Esedoglu, R. Tsai, Threshold dynamics for the piecewise constant Mumford–Shah functional, J. Comput. Phys. 211 (1) (2006) 367–384.
[15] K. Mikula, F. Sgallari, Semi-implicit finite volume scheme for image processing in 3D cylindrical geometry, J. Comput. Appl. Math. 1 (2003) 119–132.
[16] J. Lie, M. Lysaker, X.C. Tai, A binary level set model and some applications for Mumford–Shah image segmentation, IEEE Trans. Image Process. 15 (4) (2006) 1171–1181.
[17] S. Lee, J.K. Seo, Level set-based bimodal segmentation with stationary global minimum, IEEE Trans. Image Process. 15 (2006) 2843–2852.
[18] D. Mumford, J. Shah, Optimal approximation by piecewise smooth functions and associated variational problems, Commun. Pure Appl. Math. 14 (1989) 577–685.
[19] L.A. Vese, T.F. Chan, A multiphase level set framevork for image segmentation using the Mumford and Shah model, Int. J. Comput. Vis. 50 (3) (2002) 271–293.
[20] S. Osher, J.A. Sethian, Fronts propagating with curvature-dependent speed: algorithms based on Hamilton–Jacobi formulations, J. Comput. Phys. 79 (1) (1988) 12–49.
[21] L. Wang, L. He, A. Mishra, C. Li, Active contours driven by local Gaussian distribution fitting energy, Signal Process. 89 (2009) 2435–2447.
[22] G. Aubert, P. Kornprobst, Mathematical Problems in Image Processing: Partial Differential Equations and the Calculus of Variations, Springer, New York, 2002.
[23] M. Beneš, V. Chalupecký, K. Mikula, Geometrical image segmentation by the Allen–Cahn equation, Appl. Numer. Math. 51 (2004) 187–205.
[24] F. Guo, Y. Yue, B. Chen, L.J. Guo, A novel multi-scale edge detection technique based on wavelet analysis with application in multiphase flows, Powder. Technol. 202 (2010) 171–177.
[25] MATLAB Version 2009, 2009. The MathWorks, Inc.,3 Apple Hill Drive, Natick, Massachusetts 01760–2098, USA.